BONE REMODELLING AND MULTIPHYSICAL PHENOMENA

T. Lemaire *Université Paris-Est, Laboratoire Modélisation et Simulation Multi Echelle, MSME UMR 8208 CNRS, 61 Avenue du Général de Gaulle, 94010 Créteil cedex, France. Téléphone : +33 1 45 17 15 72, Télécopie : +33 1 45 17 14 33. Adresse électronique : thibault.lemaire@univ-paris-est.fr*

Mots clés :Biomechanics, Bone remodelling, Multiphysical phenomena, Multiscale analysis, Poromechanics.

1 INTRODUCTION

"Life is definable as the continuous adjustment of internal relations to external relations" [54].

The mechano-transduction process consists of a chain of three main functions : mechano-reception, mechano-transmission and mechano-activation. Whether they are biological or more generally industrial, these functions make that some systems act as mechano-sensors and/or senso-actors. Thus, these systems are able to gather and transmit information on their neighborhood and on themselves, modifying so their properties in response to various physico-chemical solicitations.
The living materials, which are intrinsically active systems, are typical adaptive systems that may change their response in function of the context. Their activity generates changes in mass, composition and shape. This phenomenon is called remodelling.
As such bone tissue can sense, react and adapt itself to its environmental vicinity [48]. For instance, it is well known that the bone quality decreases during space flight [37].
Thus bone formation and resorption is the result of a series of events transforming a physical information into a biological response. This process including all the phenomena characterizing the bone cell ability to sense mechanical *stimuli* and possibly to reply is called the mechano-transduction of bone remodelling. As sketched in Fig. 1, the cycle of bone remodelling can be coarsely summarized as : a macroscopic external physical *stimulus* (i) is propagated within the bone tissue (ii), and then sensed at the microscale by sensitive cells (typically the osteocytes, OCY) (iii), that induce signals emission (iv) to activate effector cells that will resorb (osteoclasts, OCL) old tissue and create (osteoblasts, OBL) new one (v), thus modifying the macroscopic properties of the organ (vi).
This adaptation results in the optimization of bone morphology to obtain the best mechanical resistance using the minimum mineral quantity. This was already postulated in the nineteenth century by the surgeon Julius Wolff [61].
In most of the modelling representations of bone remodelling, the physical *stimuli* acting on bone cells (pressure, shear stress, drag forces, etc.) are calculated from mechanical loading at the scale of the organ thanks to the poromechanics theory [6]. These physical inputs are then somehow downscaled and converted into biochemical microscopic signals regulating the remodelling activity [1]. In this manner, the nature of the macroscopic incoming signals is thought to be purely mechanical. Moreover, the microscopic phenomena are often not directly involved since the fluid flow around the cells is quantified by a macroscopic parameter, the hydraulic permeability for instance. In other words, even if involving microscopic biochemical signals, these modelling strategies often remain purely macroscopic.
In this contribution, we would like to emphasize recent developments that may strongly modify the current bone mechano-sensation paradigm. Using a multiscale strategy, we propose to investigate the multiphysics effects due to the physico-chemical phenomena that occur at the microstructural scale of bone tissue. In particular, we trace how the fluid-flow and mass transport models for mechano-transduction should be changed by considering additional effects related to electro-chemical couplings that characterize the cellular vicinity. Our strategy consists in discussing, at both the macroscale and the microscale, the importance of the multiphysical phenomena featuring in bone behaviour using physiologically-based simulations.

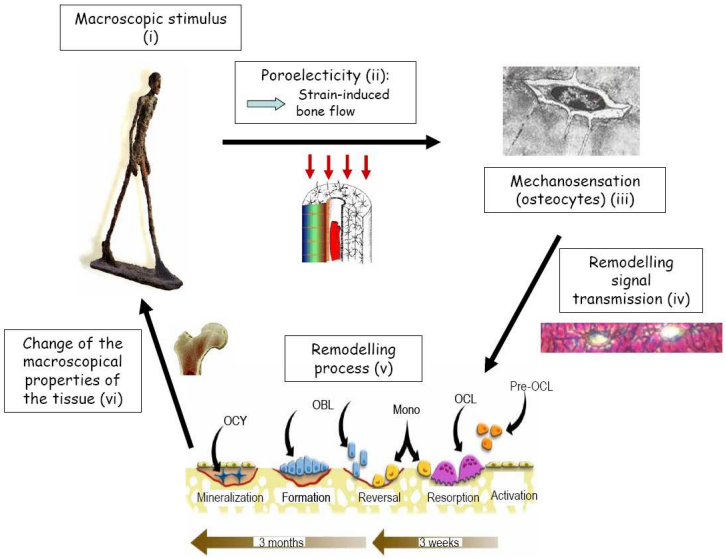

FIG. 1 – Simplified chain of the mechano-transduction of bone remodelling (reproduced with permission from [24])

2 SOME BASIC ASPECTS IN BONE PHYSIOLOGY

2.1 Structure of bone tissue

Bone is a multiscale complex structure [7, 8] presenting two types of tissue (see Fig. 2-A) : i/ the trabecular bone (or spongy bone), a very porous tissue (porosity $\sim 85\%$), located in the interior region of bone and containing bone marrow where hematopoiesis takes place ; ii/ the cortical bone (or compact bone), less porous (porosity $\sim 3\%$), located at the periphery of long bones. Representing 90% of the total bone mass, cortical tissue permits the locomotion, stores and releases chemical elements like calcium or phosphorous and protects the organs.

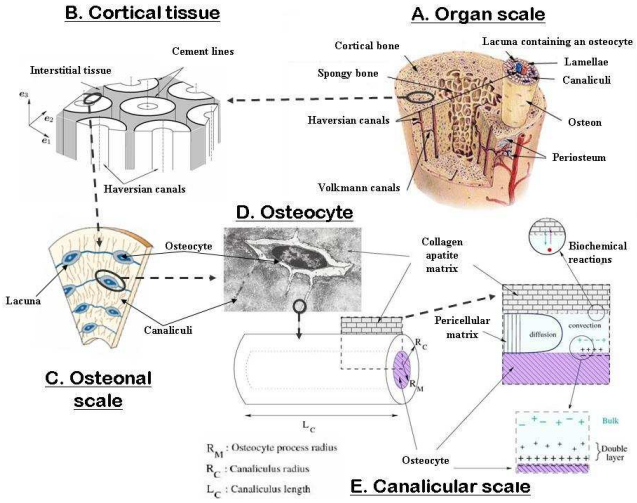

FIG. 2 – Multiscale bone structure (reproduced with permission from [24]).

The cortical unit structure, called osteon, is a cylinder whose radius is about 10^{-4} m (see Fig. 2-B). An osteon is constituted by the collagen-apatite matrix containing vascular porosity (Haversian and Volkmann's canals) and elliptic holes named *lacunae*. Each *lacuna* holds one mechanical sensor cell (osteocyte, see Fig. 2-D) swimming in fluid environments. These osteocytes develop within little channels (*canaliculi*) connecting them together and so forming a stellar network within bone volume (see Fig. 2-C). At the microscale, the representative volume is a fraction of the lacuno-canalicular system (see Fig. 2-E). Canaliculi are described by two concentric straight cylinders whose the cross section is circular with radii R_C and R_M such as $R_C > R_M$. The interstitial fluid occupies the annular space between the canalicular wall and the osteocyte process membrane. Note that the smallest porosity level in bone corresponds to the spaces inside the collagen-apatite structure (CAP, typical pore size of

5 nm). Since it is thought that at this lowest level most of the water is bound to ionic crystals [11] and plays a key role in structuring the apatite mineral [59], the water flow at this nanometric scale is often simply omitted in bone fluid flow representations, resulting in a two-fold porous treatment of bone poromechanics [12, 47, 27].

2.2 Bone remodelling signals

There has been considerable speculation that osteocytes, the mechanosensitive bone cells, produce a signal proportional to mechanical loading by sensing different remodelling signals within bone tissue through stretch-activated ion channels, interstitial fluid flow, electrical potentials, or some other phenomenon. In this subsection, the main *stimuli* that can induce bone remodelling are presented.

2.2.1 *Stimuli* originating in the solid matrix of bone. According to the Wolff's law [61] that roughly states that bone is preferentially deposited in the area characterized by a high mechanical solicitation and removed where it is not mechanically needed, the first research of the bone remodelling were linked to the skeleton deformations.

- **Bone matrix micro-strains** Considering different physical activities, micro-strains of the human skeleton have been measured thanks to micro-gauges exhibiting values ranging between 0.04 % and 0.3 % [22, 10]. The key parameters that directly influence the biological response of bone tissue have been shown to be the strain amplitude [50] and the strain rate [15, 49, 55].

- ***Hiatus* between *in vivo* and *in vitro* micro-strains** In physiological conditions typically corresponding to normal locomotion activities, the bone tissue strains that can be measured *in vivo* remain rather small since quantitative data obtained for running horses and men and fast flying birds present maximal values around $0.2 - 0.3$ % [10]. These measurements are paradoxical when compared to the *in vitro* necessary strains that induce a cellular response which are one or two order higher, from 1 to 10 % [13]. *In vivo*, such a huge strain level would cause bone fracture. This paradox reinforces the idea that the direct mechano-sensation of the mechanical loading by the bone surface cells is certainly not the main sensing pathway.

- **Micro-cracks** Notwithstanding the reversible micro-strains, physiological observations of bone tissue exhibit that normal bone presents micro-cracks [42]. These cracks originate within the bone cortex and tend to merge and propagate along the cement lines that form the outer layer of the osteons [52]. The stress concentration phenomenon that is inherent to these micro-cracks has been proposed to be the key textural phenomenon inducing the remodelling process [19]. Sites of remodelling in cortical bone have been indeed shown to occur in conjunction with microcracks [9]. In particular, it has been observed experimentally that a strong association between microdamage, osteocyte viability and modulation of remodelling activity does exist [57].
  Concomitantly, microcracks are likely to alter the fluid flow and convective transport through the bone tissue and thus modify the hydraulic behaviour of the fluid in the vicinity of the sensitive cells [14, 41].

- **Bone piezo-electricity** In the 1960s, electric measurements in bone tissue [62] motivated the hypothesis that bone adaptation could be explained thanks to collagen piezo-electricity. Historically, it was argued that a mechanically loaded bone induces compression on its concave side and tension on its convex side [4], stimulating or limiting bone formation or resorption according to the local electrical field.This piezo-electric craze faded away in the 1980s when more compelling mechanisms related to the interstitial fluid movement began being studied [17]. Only recent studies proposed that piezo-electricity could induce an increase in the electric charge of the bone tissue and thus engenders an opposite electro-osmotic flow limiting the total interstitial flow, and thus increasing the apparent stiffness and the mass transport properties of bone tissue [2, 28].

2.2.2 Bone fluid flow signals. It had been for a long time believed that the sole function of bone interstitial fluid movement in the lacuno-canalicular pores was to provide nutrients and remove wastes. The strain induced micro-flows were first proposed by [44]. However, these lacuno-canalicular micro-flows have only been experimentally observed 20 years later by tracer studies [21, 58]. This difficulty to carry out convenient *in vivo* experiments to measure hydraulic fluid velocities and interstitial fluid pressure within bone tissue motivated the model-driven investigations of the bone behaviour.

- **Evidence of the fluid flow and stretch in bone cell activity** Several studies demonstrated that bone cells are more responsive to fluid flow than to mechanical strain. For instance, the strain-induced osteoblastic response measured by [5] is 6 times lower than the flow-induced response observed by [45, 46]. When focussing on the osteocytes, if their *in vivo* sensitivity to the mechanical loading was

known in the late 1980s [53], the strong influence of the fluid shear stress induced by neighboring flow on the cellular activity was proven *in vitro* the decade after [20].

– **Pressure effects** By comparing biochemical responses of osteoblast and osteocytes when submitted to a fluid flow, it was showed that the shear stress induced by the flow was the predominant mechanical effect felt by the cells [20]. Notwithstanding this strong evidence, some studies still impute an important role of the pressure in the bone cells behaviour [39, 40].

– **Flow shear stress** In the footsteps of [44], [60] proposed that the fluid flow due to physiological loading was the primary *stimulus* that enabled osteocytes to sense and respond to their mechanical environment. Their theoretical investigation predicted shear effects induced by the fluid flow on the osteocyte process membrane of a few Pascals. This value typically corresponds to *in vitro* measurements of bone fluid shear stress [20].

– **Drag force** Ten years later, concomitantly to the progress in the imaging of the canalicular structure [64, 36], the Weinbaum's group proposed to consider the drag force exerted by the fluid flow on the pericellular matrix surrounding the cell processes as a key remodelling stimulus. These forces would be transmitted by tethering filaments and canalicular projections which connect the membrane of the cell process to the canalicular wall, generating a strain amplification of the cell membrane in the hoop direction [63].

3 MULTIPHYSICAL BEHAVIOUR FROM THE CELL VICINITY TO THE TISSUE SCALE

In this section, a summary of the key elements of our multiphysical model of cortical bone behaviour is proposed. The readers interested in going deeper into the matter are invited to study the parent papers [31, 32, 34, 23, 26, 27]. Those previous studies present how a multiphysical description of a saturated porous material at the microscale (characterised by the micro-coordinate $\mathbf{x}$ referring to a typical micro-length ℓ) is propagated at the upper scale (characterised by the macro-coordinate $\mathbf{X}$ referring to a typical macro-length L). Through the homogenization process, we are able to discriminate the variables that vary only at the macroscale, called slow variables, from the fast variables that may also vary at the microscale. The ∇ spatial operator is used to represent the gradient of a quantity $\nabla\star$ or its divergence $\nabla\cdot\star$. This operator is split into two parts $\nabla = \eta^{-1}\nabla_x + \nabla_X$, where ∇_x and ∇_X correspond to differentiations at the micro- and macroscale respectively, and where $\eta = \ell/L$ is the scaling ratio. Eventually, focussing on cortical bone analysis, the slow variables are : i) the displacement vector field of the solid skeleton $\mathbf{u}$ -this result is quite classical in homogenization theories of poroelasticity [3]- ; ii) the fluid pressure p ; iii) the salinity of the interstitial fluid n ; iv) the streaming potential ψ. In other words, $\nabla_x\mathbf{u} = \mathbf{0}$ and $\nabla_x p = \nabla_x n = \nabla_x\psi = \mathbf{0}$.
These slow variables, in association with several other fast ones, are linked through coupled equations forming the multiphysical model.

3.1 Electricity : piezoelectricity, double-layer effects and streaming potentials

3.1.1 Electricity in the collagen-apatite matrix. The piezoelectric effect is closely related to a change of polarization density within the collagen matrix. As a result, bone can be considered as a sort of dielectric material exhibiting a quasi-permanent bulk charge q_s. Let the permittivity of the solid phase be quantified by the second-order tensor $\boldsymbol{\epsilon}_s$ and the piezoelectric coupling by the the piezoelectric third-order tensor $\boldsymbol{\Pi}$. At the scale of the collagen-apatite structure, the electric potential in the solid phase ϕ_s is thus governed by the Gauss-Maxwell law :

$$\nabla\cdot(\boldsymbol{\Pi} : \nabla\mathbf{u} - \boldsymbol{\epsilon}_s\cdot\nabla\phi_s) = q_s. \tag{1}$$

Here, the two operators $\cdot$ and $:$ correspond to the single and double contractions, respectively. Electricity in the solid phase involves both the displacement vector field $\mathbf{u}$ and the electric potential in the solid ϕ_s. In fact, when homogenized, this equation remains purely microscopic [23] and, since the displacement $\mathbf{u}$ is a slow field, it only involves the electric potential :

$$-\nabla_x\cdot(\boldsymbol{\epsilon}_s\cdot\nabla_x\phi_s) = q_s. \tag{2}$$

3.1.2 Double-layer and streaming potentials in the fluid. An important property inherent to most of the biological charged porous media is the negative charge of their pore surface due to the presence of some negative sites such as hydroxyl complexes. This negative charge is partially compensated by the adsorption of cations on the surface forming the inner compact layer commonly referred to as the immobile Stern layer. Nevertheless, the majority of the excess of positively charged counter-ions is

located in the electrolyte aqueous solution forming an outer diffuse layer composed of mobile charges. Together with the fixed charged groups on the solid matrix, these ions form the so-called electric double-layer [16].
Due to the negative charge of the pore surface, the cationic and anionic concentrations $n^{\pm}$ are governed by a Boltzmann distributions involving the reduced double-layer potential $\bar{\varphi}$:

$$n^{\pm} = n \exp(\mp \bar{\varphi}). \tag{3}$$

Note that the reduction of electric potentials $\star$ involves the Faraday constant F, the ideal gas constant R and the absolute temperature T, so that $\bar{\star} = F \star / RT$. The double-layer potential φ can be determined thanks to the purely microscopic Poisson-Boltzmann equation [26] :

$$\nabla_x \cdot \nabla_x \bar{\varphi} = \frac{1}{L_D^2} \sinh \bar{\varphi}. \tag{4}$$

The Debye length $L_D = \sqrt{\epsilon_f RT/(2F^2 n)}$ characterises the thickness of the diffuse ionic layer. Here, ϵ_f is the dielectric permittivity of the fluid phase (note that the permittivity tensor in the fluid is spherical, $\boldsymbol{\epsilon}_f = \epsilon_f \mathbf{I}$, $\mathbf{I}$ being the unit second-order tensor).

3.2 Ionic electro-diffusive transport

In the remodelling process, the paracrine communication between the mechanosensors (osteocytes) and the effector cells (osteoclasts and osteoblasts) requires to develop specific transport processes. Neglecting the convective effects in the narrow *canaliculi* but taking into account the ionic exchanges, the electrical phenomena induced by the double-layer and the streaming current require to modify the classical diffusion equation. Thus, taking into account the possible ionic exchanges between the cell and its fluid environment and the electromigration effects, a macroscopic electro-diffusive Nernst-Planck equation can be obtained for monovalent ions [26] :

$$\frac{\partial}{\partial t} \left[n \left(\eta_f < \exp(\mp \bar{\varphi}) >_f + \alpha_{\mp} \right) \right] = \nabla_X \cdot \left[\mathbf{D}_{\pm}^* \left(\nabla_X n \pm n \nabla_X \bar{\psi} \right) \right]. \tag{5}$$

Here, $< \star >_f$ represents the average value of the quantity over the fluid domain. This equation exhibits three contributions to the ionic transport : i) the temporal term involving the influence of the porosity η_f, the averaged double-layer effects and the surface exchange term $\alpha_{\mp}$; ii) a Brownian diffusion term in response to the salinity gradient ; iii) an electromigration term in response to the gradient of the streaming potential ψ. These two last terms are quantified using effective diffusion tensors $\mathbf{D}_{\pm}^*$ involving, in addition to the diffusion coefficients of the ions $D_{\pm}$, the porosity η_f and the electro-tortuosity tensors $\boldsymbol{\vartheta}_{\pm}$:

$$\mathbf{D}_{\pm}^* = \eta_f D_{\pm} \boldsymbol{\vartheta}_{\pm}^{-1}. \tag{6}$$

The explicit definition of $\boldsymbol{\vartheta}_{\pm}$ is obtained during the homogenization process and can be found elsewhere [25, 23].

3.3 Interstitial fluid flow

Bone fluid flow, in addition to the hydraulic pressure gradient, may be governed by supplementary driving phenomena. Indeed, due to the variability of the streaming potential, an electrophoretic movement of the mobile charges is generated. As a result, because of the viscous drag interaction, a concomitant electro-osmotic seepage flow is caused. Moreover, the chemical gradients engender osmotic fluid movement too. In a previous study [32], a modified Darcy law taking into account electrokinetics and the fibrous pericellular matrix occupying the canalicular porosity (thanks to a pericellular matrix permeability K_f) has been derived. The strategy was to upscale the Stokes equation including the Coulombic force to show that the fluid flow is caused by three driving effects, namely hydraulic transport (induced by a pressure gradient, indexed by P), osmosis (in response to a salinity gradient, indexed by C) and electro-osmosis (caused by a streaming potential gradient, indexed by E). Hence the macroscopic Darcy velocity $\mathbf{V}$ reads :

$$\mathbf{V} = -\mathbf{K}_P \nabla_X p - \mathbf{K}_C \nabla_X n - \mathbf{K}_E \nabla_X \bar{\psi}. \tag{7}$$

The macroscopic permeability tensors $\mathbf{K}_k =< \boldsymbol{\kappa}_k >$ are obtained through the homogenization process [32, 34, 23], $< \boldsymbol{\kappa}_k >$ being the average over the representative volume of the local hydraulic conductivity parameters in response to each of the three driving effects ($k = P, C, E$).

3.4 Coupled poroelasticity

Bone fluid flow is generated by the strain of the solid matrix. Classically, in bone biomechanics, the calculation of the hydraulic velocities caused by the mechanical loading are based on the poroelasticity theory [6]. Here, we consider the extension of this purely hydro-mechanical modelling to electrically charged and saturated porous media recently developed in [23]. Thus, transposing the multiscale coupled representations of saturated clayey materials [30, 38] based on the seminal paper of [3], our strategy consists in deriving a Biot-like constitutive equation from a microscale analysis. On the one hand, the solid phase of cortical bone obeys to the piezoelectric constitutive equation :

$$\mathbf{S}_s = \mathbb{C} : \varepsilon(\mathbf{u}) + \mathbf{\Pi}^T \cdot \nabla \phi_s, \tag{8}$$

where $\mathbf{S}_s$ is the second-order stress tensor in the solid, $\star^T$ stands for the transpose operator and $\varepsilon(\star) = (\nabla \star + \nabla \star^T)/2$ is the operator that gives the symmetric part of the gradient of the quantity $\star$. This operator is also used to express the symmetric part of the interstitial fluid velocity $\mathbf{v}$ hereafter.
On the other hand, the constitutive equation for the Newtonian fluid phase involves the Donnan osmotic pressure π_D and the second-order Maxwell tensor $\boldsymbol{\tau}_M$ characterising the electrical effects :

$$\mathbf{S}_f = -(p + \pi_D)\mathbf{I} + 2\mu_f\, \varepsilon(\mathbf{v}) + \boldsymbol{\tau}_M, \tag{9}$$

where $\mathbf{S}_f$ is the stress tensor in the fluid and μ_f is the dynamic viscosity of the fluid. The osmotic pressure typically corresponds to the swelling pressure, as observed in clayey materials [35, 29] and is expressed thanks to the double-layer potential :

$$\pi_D = 2RTn(\cosh \bar{\varphi} - 1). \tag{10}$$

Furthermore, the Maxwell tensor $\boldsymbol{\tau}_M$ is defined thanks to the electric field vector in the fluid $\mathbf{E}_f$ by :

$$\boldsymbol{\tau}_M = \frac{\epsilon_f}{2}(2\mathbf{E}_f \otimes \mathbf{E}_f - (\mathbf{E}_f \cdot \mathbf{E}_f)\mathbf{I}), \tag{11}$$

$\otimes$ being the tensor product. The use of this constitutive equation in the equilibrium equation of the fluid phase simply gives the Stokes equation used to describe the interstitial fluid movement. It can be noticed that the divergence of the Maxwell tensor $\boldsymbol{\tau}_M$ simply represents the Coulombic force [38].
After upscaling, the piezoelectric effects fade away at the macroscale [23] and the overall momentum balance equation, involving the total stress tensor, $\mathbf{S_{tot}} =< \mathbf{S}_s > + < \mathbf{S}_f >$, expressed from the averaged stress tensors in the solid and fluid phases, reads :

$$\nabla_X \cdot \mathbf{S_{tot}} = \mathbf{0}. \tag{12}$$

The total stress tensor obeys to a coupled Biot-like equation explicitly derived elsewhere [23] :

$$\mathbf{S_{tot}} = \mathbb{C}^* : \varepsilon_X(\mathbf{u}) - \boldsymbol{\alpha}^* p + \boldsymbol{\tau}^*. \tag{13}$$

In this equation, ε_X corresponds to the macroscopic part of the operator ε, that is to say built from ∇_X. Furthermore, the homogenized fourth-order elasticity tensor $\mathbb{C}^*$ and the homogenized Biot second-order tensor $\boldsymbol{\alpha}^*$ are obtained following the classical treatment of poroelasticity as proposed by [3]. Moreover, the macroscopic electro-chemical tensor $\boldsymbol{\tau}^*$ representing the macroscopic effects of the fluid electro-chemical phenomena is similar to the one previously obtained for the multiphysical description of clayey materials [30, 38]. This tensor accounts for : i) the spherical Donnan pressure effect ; ii) the action of the Maxwell tensor ; iii) the electro-chemical effects occurring at the solid-fluid interface [23].

4 CONSEQUENCES ON BONE REMODELLING SIGNALS

This model of bone behaviour was used to highlight the effects of multiphysical phenomena on bone physiology [18, 51].
Adopting the multiscale approach extensively presented in [23], we showed that a classical treatment of the bone behaviour only involving the hydro-mechanical effects is more or less sufficient to recover the bone hydro-mechanical macroscopic behaviour [24]. In fact, the electro-chemical phenomena being originated by the electric charge of the solid-fluid interface, the canalicular pores are large enough to limit their consequences at the tissue level. The double-layer and piezoelectric effects are thus purely microscopic. They only slightly modify the macroscopic ionic transport, whereas the behaviour of bone can be fairly well described by classical poroelasticity combined with the usual Darcy law.

Consequently, classical bone modelling efforts involving poroelasticity adequately evaluate the fields associated with the fluid phase (pressure field, Darcian velocity, etc.) at the tissue level.
Notwithstanding this efficiency of classical macroscopic approaches, they ignore the phenomena occurring at the cell scale. In particular, the mechanotransduction of the remodelling signals, which is microscopic by nature, is often only represented through *ad hoc* macroscopic laws [1, 56]. In consequence, the electro-chemical effects located at the cellular level are simply left aside. Even if invisible at the tissue scale, the microscopic implications of electro-chemistry in the cellular mechanosensation cannot be neglected since we showed that electro-chemically driven fluid shear stress inducing a bone cells response could be obtained [18]. Indeed, the electro-chemical contributions to the local fluid signals are more important near the cell membrane where the double-layers develop. As a result, a purely macroscopic description of bone remodelling provides a somewhat skewed representation of the *in vivo* remodelling signals.

5 CONCLUSIONS AND PROSPECTS

Through the poromechanical coupling, the correlation between interstitial bone fluid flow and the skeleton mechanical sollicitations is the key element to understand the mechanoadaptation ability of this organ. Since the experimental description of the fluid flow within the bone tissue is still a very challenging topic [28, 11], theoretical approaches are often carried out to understand the in vivo phenomena that govern bone behaviour. With our multiscale and multiphysical approach, we have been able to put into relief the necessity to consider electro-chemical phenomena in the bone cells activity. Even if washed out at the tissue level, these microscopic electro-chemical signals remain important in the neighbourhood of the cells.
Our current avenue of research is now to question another classical assumption in the bone fluid flow induced mechanotransduction : the nanopores of the collagen-apatite matrix are too small to contain free water, and thus to participate to bone fluid flow. Using molecular dynamics approaches, we recently showed that this assumption may be doubtful since we were able to simulate nanoscopic Poiseuille-like profiles in hydroxy-apatite pores of a few nanometers [43, 33].

Références

[1] T. Adachi, Y. Kameo, and M. Hojo. Trabecular bone remodelling simulation considering osteocytic response to fluid-induced shear stress. *Philosophical Transactions of the Royal Society A*, 368 :2669–2682, 2010.

[2] A.C. Ahn and A.J. Grodzinsky. Relevance of collagen piezoelectricity to wolff's law : A critical review. *Medical Engineering & Physics*, 31 :733–741, 2009.

[3] J. L. Auriault and E. Sanchez-Palencia. Etude du comportment macroscopique d'un milieu poreux saturé déformable. *Journal de Mécanique*, 16 :575–603, 1977.

[4] C.A. Bassett, R.J. Pawluk, and R.O. Becker. Effects of electric currents on bone in vivo. *Nature*, 204 :652–654, 1964.

[5] I. Binderman, Z. Shimshoni, and D. Somjen. Biochemical pathways involved in the translation of physical stimulus into biological message. *Calcif. Tissue Int.*, 36 :S82–85, 1984.

[6] M. A. Biot. General theory of three-dimensional consolidation. *Journal of Applied Physics*, 12 :155–164, 1941.

[7] J.A. Buckwalter, M.J. Glimcher, R.R. Cooper, and R. Recker. Bone biology. Part I : Structure, blood supply, cells, matrix, and mineralization. *J. Bone Joint Surg. - Am.*, 77 :1256–1275, 1995.

[8] J.A. Buckwalter, M.J. Glimcher, R.R. Cooper, and R. Recker. Bone biology. Part II : Formation, form, modeling, remodeling, and regulation of cell function. *J. Bone Joint Surg. - Am.*, 77 :1276–1289, 1995.

[9] D.B. Burr and R.B. Martin. Calculating the probability that microcracks initiate resorption spaces. *J. Biomech.*, 26 :613–616, 1993.

[10] D.B. Burr, C. Milgrom, D. Fyhrie, Forwood M., M. Nyska, A. Finestone, S. Hoshaw, E. Saiag, and A. Simkin. In vivo measurement of human tibial strains during vigorous activity. *Bone*, 18 :405–410, 1996.

[11] L. Cardoso, S.P. Fritton, G. Gailani, M. Benalla, and S.C. Cowin. Advances in assessment of bone porosity, permeability and interstitial fluid flow. *J. Biomech.*, 46 :253–265, 2013.

[12] S.C. Cowin, G. Gailani, and M. Benalla. Hierarchical poroelasticity : movement of interstitial fluid between porosity levels in bones. *Philos. T. R. Soc. A*, 367 :3401–3444, 2009.

[13] S.P. Fritton, K.J. Mcleod, and C.T. Rubin. Quantifying the strain history of bone : spatial uniformity and self-similarity of low-magnitude strains. *J. Biomech.*, 33 :317–325, 2000.

[14] S.A. Galley, D.J. Michalek, and S.W. Donahue. A fatigue microcrack alters fluid velocities in a computational model of interstitial flow in cortical bone. *J. Biomech.*, 39 :2026–2033, 2006.

[15] J. Hert, M. Liskova, and J. Landa. Reaction of bone to mechanical stimuli. 1.continuous and intermittent loading of tibia in rabbit. *Folia Morphol.*, 19 :290–300, 1971.

[16] R.J. Hunter. *Zeta Potential in Colloid Science : Principles and Applications.* Academic Press, 1981.

[17] M. W. Johnson, D. A. Chakkalakal, R. A. Harper, J. L. Katz, and S. W. Rouhana. Fluid flow in bone in vitro. *J. Biomech.*, 15 :881–885, 1982.

[18] J. Kaiser, T. Lemaire, S. Naili, V. Sansalone, and S.V. Komarova. Do calcium fluxes within cortical bone affect osteocyte mechanosensitivity ? *J. Theoret. Biol.*, 303 :75–86, 2012.

[19] S. Kasiri and D. Taylor. A critical distance study of stress concentrations in bone. *J. Biomech.*, 41 :603–609, 2008.

[20] J. Klein-Nulend, A. van der Plas, C. M. Semeins, N. E. Ajubi, J. A. Frangos, P. J. Nijweide, and E. H. Burger. Sensitivity of osteocytes to biomechanical stress *in vitro*. *Faseb J.*, 9 :441–445, 1995.

[21] M.L. Knothe Tate, R. Steck, M.R. Forwood, and P. Niederer. In vivo demonstration of load-induced fluid flow in the rat tibia and its potential implications for processes associated with functional adaptation. *J. Exp. Biol.*, 203 :2737–2745, 1998.

[22] L.E. Lanyon, W.G. Hampson, A.E. Goodship, and J.S. Shah. Bone deformation recorded in vivo from strain gauges attached to the human tibial shaft. *Acta Orthop. Scand.*, 46 :256–268, 1975.

[23] T. Lemaire, E. Capiez-Lernout, J. Kaiser, S. Naili, E. Rohan, and V. Sansalone. A multiscale theoretical investigation of electric measurements in living bone. Piezo-electricity and electrokinetics. *Bull. Math. Biol.*, 73 :2649–2677, 2011.

[24] T. Lemaire, E. Capiez-Lernout, J. Kaiser, S. Naili, and V. Sansalone. What is the importance of multiphysical phenomena in bone remodelling signals expression ? a multiscale perspective. *Journal of the mechanical behavior of biomedical materials*, 4 :909–920, 2011.

[25] T. Lemaire, J. Kaiser, S. Naili, and V. Sansalone. Modelling of the transport in charged porous media including ionic exchanges. *Mechanics Research Communications*, 37 :495–499, 2010.

[26] T. Lemaire, J. Kaiser, S. Naili, and V. Sansalone. Textural versus electrostatic exclusion-enrichment effects in the effective chemical transport within the cortical bone : A numerical investigation. *Int. J. Num. Meth. Biomed. Eng.*, 29 :1223–1242, 2013.

[27] T Lemaire, J Kaiser, S Naili, and V Sansalone. Three-scale multiphysics modeling of transport phenomena within cortical bone. *Mathematical Problems in Engineering*, 2015 :398970, 2015.

[28] T. Lemaire, S. Lemonnier, and S. Naili. On the paradoxical determinations of the lacuno-canalicular permeability of bone. *Biomechanics and modeling in mechanobiology*, 11(7) :933–946, 2012.

[29] T. Lemaire, C. Moyne, and D. Stemmelen. Imbibition test in a clay powder (mx-80 bentonite). *Applied Clay Science*, 26 :235–248, 2004.

[30] T. Lemaire, C. Moyne, D. Stemmelen, and M.A. Murad. Electro-chemo-mechanical couplings in swelling clays derived by homogenization : electroviscous effects and onsager's relations. In *Poromechanics II*, pages 489–500. Balkema Publishers, Lisse, 2002.

[31] T. Lemaire, S. Naili, and A. Rémond. Multi-scale analysis of the coupled effects governing the movement of interstitial fluid in cortical bone. *Biomechanics and Modeling in Mechanobiology*, 5 :39–52, 2006.

[32] T. Lemaire, S. Naili, and A. Rémond. Study of the influence of fibrous pericellular matrix in the cortical interstitial fluid movement. *Journal of Biomechanical Engineering*, 130 :11001,1–11, 2008.

[33] T. Lemaire, T.T. Pham, E. Capiez-Lernout, N.H. de Leeuw, and S. Naili. Water in hydroxyapatite nanopores : possible implications for interstitial bone fluid flow. *J. Biomech*, 48 :3066–3071, 2015.

[34] T. Lemaire, V. Sansalone, and S. Naili. Multiphysical modelling of fluid transport through osteoarticular media. *Annals of the Brazilian Academy of Sciences*, 82 :127–144, 2010.

[35] P.F. Low. The clay/water interface and its role in the environment. *Progress in Colloid and Polymer Science*, 95 :98–107, 1994.

[36] L.M. McNamara, R.J. Majeska, S. Weinbaum, V. Friedrich, and M.B. Schaffler. Attachment of osteocyte cell processes to the bone matrix. *Anat. Rec.*, 292 :355–363, 2009.

[37] E.R. Morey and D.J. Baylink. Inhibition of bone formation during space flight. *Science*, 201 :1138–1141, 1978.

[38] C. Moyne and M. A. Murad. Electro-chemo-mechanical couplings in swelling clays derived from a micro/macro-homogenization procedure. *International Journal of Solids and Structures*, 39 :6159–6190, 2002.

[39] J. Nagatomi, B.P. Arulanandam, D.W. Metzger, A. Meunier, and R. Bizios. Frequency- and duration-dependent effects of cyclic pressure on select bone cell functions. *Tissue Eng*, 7 :717–728, 2001.

[40] J. Nagatomi, B.P. Arulanandam, D.W. Metzger, A. Meunier, and R. Bizios. Effects of cyclic pressure on bone marrow cell cultures. *J. Biomech. Eng.*, 124 :308–314, 2002.

[41] V.-H. Nguyen, T. Lemaire, and S. Naili. Influence of interstitial bone microcracks on strain-induced fluid flow. *Biomech. Model. Mechanobiol.*, 10 :963–972, 2011.

[42] F.J. O'Brien, D. Taylor, G.R. Dickson, and T.C. Lee. Visualisation of three-dimensional microcracks in compact bone. *Journal of Anatomy*, 197 :413–420, 2000.

[43] T.T. Pham, T. Lemaire, E. Capiez-Lernout, M. Lewerenz, Q.-D. To, J.K. Christie, D. Di Tommaso, N.H. de Leeuw, and S. Naili. Properties of water confined in hydroxyapatite nanopores as derived from molecular dynamics simulations. *Theoret. Chem. Acc.*, 134 :59, 2015.

[44] K. Piekarski and M. Munro. Transport mechanism operating between blood supply and osteocytes in long bones. *Nature*, 269 :80–82, 1977.

[45] K.M. Reich and J.A. Frangos. Effect of flow on prostaglandin e2 and inositol triphosphate levels in osteoblasts. *Am. J. Physiol.*, 261 :C428–432, 1991.

[46] K.M. Reich and J.A. Frangos. Protein kinase c mediates flow-induced prostaglandin e2 production in osteoblasts. *Calcif. Tissue Int.*, 52 :62–66, 1993.

[47] E. Rohan, S. Naili, R. Cimrman, and T. Lemaire. Multiscale modeling of a fluid saturated medium with double porosity : Relevance to the compact bone. *Journal of the Mechanics and Physics of Solids*, 60(5) :857–881, 2012.

[48] N. Rosa, R. Simoes, F. Magalhães, and A.T. Marques. From mechanical stimulus to bone formation : A review. *Medical engineering & physics*, 37 :719–728, 2015.

[49] C.T. Rubin and L.E. Lanyon. Limb mechanics as a function of speed and gait : a study of functional strains in the radius and tibia of horse and dog. *J. Exp. Biol.*, 101 :187–211, 1982.

[50] C.T. Rubin and L.E. Lanyon. Regulation of bone mass by mechanical strain magnitude. *Calcif. Tissue Int.*, 37 :411–417, 1985.

[51] V. Sansalone, J. Kaiser, S. Naili, and T. Lemaire. Interstitial fluid flow within bone canaliculi and electro-chemo-mechanical features of the canalicular milieu : A multi-parametric sensitivity analysis. *Biomech. Model. Mechanobiol*, 12 :533–553, 2013.

[52] M.B. Schaffer, K. Choi, and C. Milgrom. Aging and matrix microdamage accumulation in human compact bone. *Bone*, 17 :521–525, 1995.

[53] T.M. Skerry, L. Bitenski, J. Chayen, and L.E. Lanyon. Early strain-related changes in enzyme activity in osteocytes following bone loading *in vivo*. *J. Bone Miner. Res.*, 4 :783–788, 1989.

[54] H. Spencer. *First Principles*. Williams and Norgate, 2nd ed., London, 1867.

[55] C.H. Turner, T. Yoshikawa, M.R. Forwood, T.C. Sun, and D.B. Burr. High frequency components of bone strain in dogs measured during various activities. *J. Biomech.*, 28(1) :39–44, 1995.

[56] R. van Oers, B. van Rietbergen, K. Ito, P. Hilbers, and R. Huiskes. A sclerostin-based theory for strain-induced bone formation. *Biomechanics and Modeling in Mechanobiology*, 10(5) :663–670, 2011.

[57] O. Verborgt, N.A. Tatton, R.J. Majeska, and M.B. Schaffler. Spatial distribution of bax and bcl-2 in osteocytes after bone fatigue : Complementary roles in bone remodeling regulation ? *J. Bone Miner. Res.*, 17 :907–914, 2002.

[58] L. Wang, Y. Wang, H. Han, S. C. Henderson, R. J. Majeska, S. Weinbaum, and M. B. Scaffler. *In situ* measurement of solute transport in the bone lacunar-canalicular system. *P. Natl Acad. Sci. USA*, 102 :11911–11916, 2005.

[59] Y. Wang, S. Van Euw, F.M. Fernandes, S. Cassaignon, M. Selmane, G. Laurent, G. Pehau-Arnaudet, C. Coelho, L. Bonhomme-Coury, M.-M. Giraud-Guille, F. Babonneau, T. Azaïs, and N. Nassif. Water-mediated structuring of bone apatite. *Nature Materials*, 12 :1144–1153, 2013.

[60] S. Weinbaum, S. C. Cowin, and Y. Zeng. A model for the excitation of osteocytes by mechanical loading-induced bone fluid shear stresses. *Journal of Biomechanics*, 27 :339–360, 1994.

[61] J. Wolff. *Das Gesetz der Transformation der Knochen*. Hirschwald, Berlin, 1892.

[62] I. Yasuda. Piezoelectricity of living bone. *Journal of Kyoto Prefectural University of Medicine*, 53 :2019–2024, 1964.

[63] L. You, S. C. Cowin, M. B. Schaffler, and S. Weinbaum. A model for strain amplification in the actin cytoskeleton of osteocytes due to fluid drag on pericellular matrix. *Journal of Biomechanics*, 34 :1375–1386, 2001.

[64] L. D. You, S. Weinbaum, S. C. Cowin, and M. B. Schaffler. Ultrastructure of the osteocyte process and its pericellular matrix. *The Anatomical Record A*, 278A(2) :505–513, 2004.